Check for updates

METEOROLOGICAL APPLICATIONS
Meteorol. Appl. **25**: 406–413 (2018)
Published online 1 February 2018 in Wiley Online Library
(wileyonlinelibrary.com) DOI: 10.1002/met.1708

The high-impact 2007 hot summer over Turkey: atmospheric-blocking and heat-wave episodes

Meral Demirtaş*
Department of Meteorology, University of Ondokuz Mayıs, Samsun, Turkey

ABSTRACT: The 2007 summer was extraordinary in the Balkans and Turkey, with the region experiencing a very hot summer in numerous places, setting all-time maximum temperature records and suffering destructive fires. The heat wave exhibited daily maximum temperature anomalies in excess of 14 °C in some cities. These high-temperature anomalies can be related to a number of concurrent atmospheric and physical factors that induce persistent anticyclones, sea-surface temperature anomalies, reduced precipitation and depleted soil moisture. Prominent atmospheric factors conducive to heat-wave events can serve as a dynamic fingerprint and yield insight into their most important triggering and driving mechanisms. The prolonged atmospheric-blocking high meandering over the central Mediterranean orchestrated the atmospheric circulation and led to the advection of warm air from North Africa to the Balkans and Turkey. The associated large-scale subsidence and clear-sky conditions resulted in temperatures surpassing 40 °C at many places. Atmospheric and physical conditions contributed positively to the very high temperatures and led to two major heat-wave episodes in June and July. Atmospheric-blocking analysis revealed that two blocking episodes accompanied these heat waves. Results from this analysis indicate that the atmospheric blocking was likely responsible for establishing and maintaining the hot-weather conditions. The summer of 2007 may be considered as a strong indicator of what Turkish summers may become in future.

KEY WORDS heat wave; atmospheric blocking; climate variability; Mediterranean; Turkey; 2007

Received 1 May 2017; Revised 23 August 2017; Accepted 24 October 2017

1. Introduction

Heat wave (HW) events have discernible impacts on health, well-being, efficiency, rise in mortality and morbidity, an increased demand on energy and water supply, agricultural resources, the retail industry, ecology and tourism, increased air pollution due to wildfires, and economic consequences due to crop failure and wild forest fires.

In recent decades, high-impact heat wave events (HIHWEs) have been observed frequently: the 2003 European HW (Schär *et al.*, 2004), the 2006 HW of Central Europe (Rebetez *et al.*, 2009), the 2007 summer HIHWE of South-Eastern Europe (Founda and Giannakopoulos, 2009), and the 2010 HW of Russia (Barriopedro *et al.*, 2011). The HIHWE of 2003 led to about 70 000 deaths; the HIHWE of 2010 caused a death toll of 55 000 due to high heat and poor air quality caused by wildfires, an annual crop failure of about 25%, around 1 million ha of burned areas, and approximately US$15 billion of total economic loss (Barriopedro *et al.*, 2011).

The summer of 2007 was very hot in the Balkans and Turkey, with the region experiencing a very hot summer and numerous places setting all-time maximum temperature records (Cheval *et al.*, 2008; Founda and Giannakopoulos, 2009). The 2007 HW affected Turkey to the extent that previous records for June–July maximum temperatures observed in the past 65 years were broken in many locations during both months, according to the Turkish State Meteorological Service. On a single-day basis, 34 cities broke all-time highest temperature records, 16 of which had a daily maximum temperature over 40 °C, six of which had record-breaking temperatures in both June and July, and exceedences reached more than 10 °C in 26 cities. These extreme temperatures occurred on 24–28 June and 25–27 July 2007. The 2007 HW prompted over 130 fires in the Southeastern Europe and Mediterranean areas (WMO, 2007). In Turkey, the total burnt area reported for 2007 was 11 664 ha. In the top 10 world natural disasters for 2007 by number of casualties, the 2007 HW ranks fifth, causing 567 deaths in Southern Europe and the Balkans (Scheuren *et al.*, 2008).

HWs may be investigated from a climatological perspective, but in fact they are meteorological events governed by the temporal and spatial scales over which they occur (Perkins, 2015). The dynamic and physical factors that work in concert have been studied extensively. There is one common atmospheric dynamic ingredient in HW composition: persistent anticyclones. It is also referred to as atmospheric blocking or a persistent high, which is a stationary system that remains in place for several days and triggers and maintains a HW. There are also lower-latitude blocking highs (Marshall *et al.*, 2014), which are generally located 10° equator-ward of the classical atmospheric-blocking region, where the subtropical ridge persists during summer (Perkins, 2015). Blocking highs may be co-located (Pfahl and Wernli, 2012) or adjacent to the HW region (Marshall *et al.*, 2014), advecting hot air masses from very hot places. In a classical atmospheric-blocking event, cooler air on the poleward side does not penetrate into the equatorial side due to the blocking, and over time the warm air builds up, as in the 2003 European (Black *et al.*, 2004) and 2010 Russian HWs (Matsueda, 2011). Under persistent anticyclonic conditions, exposed to sunnier and

* Correspondence: M. Demirtaş, Department of Meteorology, University of Ondokuz Mayıs, 19 Mayıs, 55420 Samsun, Turkey. E-mail: mdemirtas@omu.edu.tr

© 2018 Royal Meteorological Society

drier air, soil moisture depletes. Dry soils inhibit cloud formation, increasing incoming solar radiation, and thus amplifying evaporation. Modelling studies of the 2003 HIHWE revealed a high sensitivity to soil-moisture conditions (Fischer *et al.*, 2007; Vautard *et al.*, 2007; Lorenz *et al.*, 2010; Miralles *et al.*, 2014). High sea-surface temperatures (SST) also have the potential to generate and sustain anticyclones. The 2003 HIHWE was found to be associated with a record-breaking warm SST of the Mediterranean Sea (Black *et al.*, 2004; Feudale *et al.*, 2007).

HWs over the Balkans and Turkey were reported to be associated with persistent anticyclones by previous studies (Founda and Giannakopoulos, 2009; Erlat and Türkeş, 2013; Unal *et al.*, 2013), but this relationship has not yet been investigated explicitly. The present study is tailored to associate HW episodes and atmospheric circulation features in an event-based approach on a grid-point basis.

The goals of this study are: (1) to determine and analyse spatiotemporal distribution, duration and intensity of the 2007 HW, using an objective HW-detection method that aims to explore the salient features of HWs; (2) to detect and analyse atmospheric-blocking episodes using a two-dimensional blocking index; and (3) to synthesize the underlying atmospheric and physical conditions that paved the way for the 2007 HW. Particular attention is paid to the dynamic link between the large-scale flow and HWs.

2. Methods

The ERA-Interim (EI) reanalysis data of the European Centre for Medium-Range Weather Forecasts (ECMWF) (Dee *et al.*, 2011) were employed with a 1° × 1° longitude–latitude grid-horizontal resolution. In order to analyse the 2007 HW from a dynamic point of view, the mean of the 500 hPa geopotential height and temperature at 2 m height, i.e. for 24–28 June and 20–27 July 2007, were computed. Composite anomalies of geopotential height at 500 hPa and temperature anomalies at 2 m were computed by removing June–July 1979–1999 climatological means. The positive anomalies of 500 hPa geopotential height were a good indication of anticyclonic conditions at the surface.

2.1. Heat wave detection method

Record-breaking temperatures should not be misled for HWs. The definition of a HW is not straightforward (Robinson, 2001), and there is no objective and uniform definition for it (Meehl and Tebaldi, 2004; Perkins, 2015). An easy and simple approach to identify a HW is based on a daily maximum temperature being above a fixed absolute threshold. A detection based on exceeding an absolute temperature threshold cannot be applied to all regions, because each region is often characterized by different microclimatic conditions. For example, in cooler areas, absolute thresholds may not be achieved, and temperatures may have to be even higher in hotter areas. In order to reduce the degree of arbitrariness involved in the selection of a threshold temperature and to provide a dynamic definition, which may also be easily transferable to other places, percentiles turn out to be more appropriate. The choice of percentiles differs in various studies: 90th (Beniston, 2004; Lorenz *et al.*, 2010; Unal *et al.*, 2013; Russo *et al.*, 2014; Spinoni *et al.*, 2015), 95th (Kuglitsch *et al.*, 2010; Founda and Giannakopoulos, 2009; Stefanon *et al.*, 2012), and 99th (Pfahl and Wernli, 2012). Percentile-based threshold temperature can be: (1) static, which does not change throughout the study period (Beniston, 2004; Founda and Giannakopoulos, 2009; Unal *et al.*, 2010); (2) dynamic, in which the temperature changes according to the respective calendar day (RCD) – it is computed at the centre of a desired time window: 31 day (Russo *et al.*, 2014), 21 day (Stefanon *et al.*, 2012), 15 day (Kuglitsch *et al.*, 2010; Spinoni *et al.*, 2015), and 5 day (Lorenz *et al.*, 2010).

The present study deals with spatial distributions and uses a non-parametric method to determine a spatially and temporally varying temperature threshold, which is based on a 95th percentile from a seven-day time window. The 95th percentile temperature threshold was computed on a grid-point basis as outlined below:

1. spatially and daily varying temperature threshold: for a given grid point, a temperature value with respect to the climatology (1979–1999) is considered to be extreme when it is above the 95th percentile. The threshold is computed for an RCD using the temperature data of the period 1979–1999 between day $d-3$ and $d+3$. For example, on 7 July, the temperatures between 4 and 10 July of 1979–1999 are used. For each day of June–July 2007, the 95th percentile was computed from a sample of seven days (three days on each side of the RCD) using Equation (1);

$$T_{(i,j,d)\text{threshold},\,95^{\text{th}}} = \bigcup_{y=1979}^{1999} \bigcup_{t=d-3}^{d+3} T_{(i,j,y,d)} \qquad (1)$$

   where $T_{(i,j,d)\text{threshold},\,95^{\text{th}}}$ is the computed temperature threshold at the 95th percentile; $\bigcup$ denotes the union of sets; and $T_{(i,j,y,d)}$ is the daily maximum temperature at 2 m height belonging to the RCD in the year (y). The indices i,j,y,d represent latitude, longitude, year and day, respectively;
2. temporal threshold: the above-described temperature threshold is to be satisfied on three consecutive days;
3. heat wave detection: a hot spell that satisfies (1) and (2) is identified as a HW;
4. heat wave severity: quantified by adding absolute temperature departures from the threshold temperature of each grid point and accumulated for the total duration of a HW (Spinoni *et al.*, 2015), and
5. heat wave intensity: computed by summing the absolute differences between the temperatures and the temperature threshold for the duration of the event; the sum is then divided by the duration of a HW (Spinoni *et al.*, 2015).

2.2. Two-dimensional atmospheric-blocking detection method

Blocking anticyclones are related to the blocking of the mid-latitude westerly atmospheric flow. They act to divert the eastward-travelling cyclones to their north or south. Blocking may cause anomalous hot and dry weather underneath the block and increased storm activity and precipitation around the block (Rex, 1950). The role played by strong-blocking anticyclones in some HW events such as the 2003 European (Black *et al.*, 2004) and 2010 Russian HWs (Matsueda, 2011), and with climatological studies on circulation anomalies during warm spells (Meehl and Tebaldi, 2004) and cold spells (Pfahl and Wernli, 2012; Demirtaş, 2017) revealed their importance. In order to diagnose atmospheric blocking objectively, it is vital to employ an objective blocking-detection technique. A two-dimensional index based on the reversal of the meridional gradient of geopotential height at 500 hPa is implemented (Tibaldi and Molteni, 1990; Scherrer *et al.*, 2006; Davini *et al.*, 2012). For every grid point of co-ordinates, the following metric

© 2018 Royal Meteorological Society

14698080, 2018, 3, Downloaded from https://rmets.onlinelibrary.wiley.com/doi/10.1002/met.1708 by NASA Shared Services Center (NSSC), Wiley Online Library on [26/05/2025]. See the Terms and Conditions (https://onlinelibrary.wiley.com/terms-and-conditions) on Wiley Online Library for rules of use; OA articles are governed by the applicable Creative Commons License

is defined:

$$GHGS\left(\lambda_0,\Phi_0\right)=\frac{Z500\left(\lambda_0,\Phi_0\right)-Z500\left(\lambda_0,\Phi_S\right)}{\Phi_0-\Phi_S} \quad (2)$$

$$GHGN\left(\lambda_0,\Phi_0\right)=\frac{Z500\left(\lambda_0,\Phi_N\right)-Z500\left(\lambda_0,\Phi_0\right)}{\Phi_N-\Phi_0} \quad (3)$$

$$\Phi_s=\Phi_0-15^{\circ} \quad (4)$$

$$\Phi_N=\Phi_0+15^{\circ} \quad (5)$$

where $Z(\lambda_0,\Phi_0)$ represents the grid point 500 hPa geopotential height at longitude (λ_0), which ranges from 0 to 360°, and latitude (Φ_0), which ranges from 30 to 70° N. The local instantaneous blocking is assigned for a location if both of the following conditions are satisfied:

$$GHGS\left(\lambda_0,\phi_0\right)\succ 0 \text{ and } GHGN\left(\lambda_0,\phi_0\right)\prec -10\,\mathrm{m}/^{\circ}\text{latitude} \quad (6)$$

A grid point is considered as large-scale blocking (LSB) if the above criteria are satisfied for at least 15 continuous longitudes. A time scale of four days is used to define a blocking episode following the work of Tibaldi and Molteni (1990).

3. Results

3.1. Mean atmospheric circulation and flow anomalies

The nature of HW episodes and their origins are tied to upper-level atmospheric dynamics and physical factors. The mean circulation of the middle troposphere during the HW episodes under consideration may illustrate the key atmospheric factors responsible for the triggering and driving mechanisms of HWs. Figures 1(a, b) illustrates the mean 500 hPa geopotential height of the two major HW episodes for the 24–28 June and 20–27 July 2007 respectively which highlights the panoply of large-scale weather systems. The prevalence of a southwest–northeast-oriented long wave ridge over the Mediterranean and a low to its northwest orchestrates the atmospheric circulation. The stationary ridge blocked cooler air on the northwest and prevented it moving towards the south to cool the HW-affected region. The ridge put the affected region under persistent southerly wind conditions. The weather was dominated by anomalous anticyclonic conditions throughout both HW episodes, with a displacement of the subtropical Azores anticyclone, extending from the Mediterranean to Western Turkey, and an intensive westerly flow on its poleward flank over the UK (as shown in Figure S1 in the supplemental data online). The atmospheric circulation at 500 hPa led to the horizontal advection of warm air masses from North Africa to the eastern Mediterranean and towards Turkey (not shown). In addition to horizontal temperature advection towards the area, the anticyclonic circulation also provided subsidence.

The spatial distribution of the composite anomalies (with respect to the 1979–1999 climatological mean) of the 500 hPa geopotential height anomaly field for both HW episodes suggests that the Azores anticyclone has been displaced towards the north. These atmospheric anomalies are the consequences of large-scale flow climate variability. Anomalies over the region exceed 100 gpm, which indicates that these large values are due to the steady residence of the same atmospheric circulation system over the area (Figures 1(c, d)). The steadiness of the anticyclone caused air to be trapped within it and travel a very short distance. Subsidence would tend to suppress convection, thus maintaining clear-sky conditions, which leads to strong heating at the surface, and reduced precipitation (as shown in Figure S2 in the supplemental data online).

A model simulation study of the winter 2007 revealed that the period from September 2006 to February 2007 was the warmest in Europe, the Balkans and Turkey, with pronounced negative precipitation anomalies over the entire Mediterranean (Luterbacher *et al.*, 2007). Dried soils emit more sensible heat flux and less latent heat flux. This leads to reduced cloudiness and, hence, further increasing diurnal surface air temperature (Black *et al.*, 2004). The land radiation budget and water resources are interrelated *via* the latent heat flux associated with evaporation. Lack of soil moisture enhances diurnal hot air entrainment and causes the formation of persistent residual layers that produce the heat that has built up (Miralles *et al.*, 2014). Modelling studies of the 2003 HW revealed a high sensitivity to soil moisture conditions (Fischer *et al.*, 2007; Vautard *et al.*, 2007; Miralles *et al.*, 2014). Analyses of June–July 2007 mean soil water content and composite anomalies (with respect to 1979–1999) revealed reduced soil moisture (as shown in Figure S3 in the supplemental data online).

Model-simulation studies of the 2003 HW (Feudale and Shukla, 2010) suggested that SST anomalies may lead to geopotential height anomalies, and they may sustain the anomalous anticyclonic circulation which causes subsiding motions and, thus, clear-sky radiative-forcing conditions (Pfahl and Wernli, 2012). Analysis of the June–July 2007 mean SST and composite anomalies (with respect to 1979–1999) (as shown in Figure S4 in the supplemental data online) indicates warm anomalies of around 4 °C over the central Mediterranean, Aegean Sea and Black Sea for June 2007. Large SST anomalies for the Mediterranean were also noted in recent studies (Miralles *et al.*, 2014; Demirtaş, 2016). It is plausible that large SST anomalies over the Mediterranean, Aegean Sea and Black Sea might have played a role in driving and maintaining the 2007 HW.

The mean 2 m temperature distribution for 24–28 June 2007 shows the largest values (36–42 °C) over the western part of Turkey (Figure 2(a)). The composite anomaly (with respect to 1979–1999) of 2 m temperature exceeds 12–16 °C, and extends over the midland (Figure 2(b)). This indicates that mean temperatures for 24–28 June 2007 are highly above the climatological mean for June. These temperature anomalies are in line with the position and magnitude of 500 hPa geopotential height anomalies (Figure 1(b)), which is located over the western side of Turkey and the June 2007 SST anomalies (as shown in Figure S4 in the supplemental data online) which are located on the northern side of the Aegean Sea and western Black Sea.

During 20–28 July 2007, temperatures are higher than those of the June period, and cover a larger area (Figure 2(c)). The composite temperature anomaly of July 2007 is also high (12–16 °C), but in some places lower than that of June 2007 (Figure 2(d)). It should be noted that the position and magnitudes of atmospheric and physical factors (Figures 1(c, d) and S1 in the supplemental data online) differ from the June 2007 period. While the SST anomalies of July 2007 are lower than the June SST anomalies, the duration of atmospheric blocking is longer in the July episode.

The impact of warm advection is seen in composite temperature anomalies which are on average 12–16 °C in June and July (Figures 2(b–d)). In order to quantify their amplitude better, normalized temperature anomalies relative to the standard deviation(s) of the 1979–1999 period were computed for the June–July 2007 period. Analyses of June–July 2007-normalized

© 2018 Royal Meteorological Society

14698080, 2018, 3, Downloaded from https://rmets.onlinelibrary.wiley.com/doi/10.1002/met.1708 by NASA Shared Services Center (NSSC), Wiley Online Library on [26/05/2025]. See the Terms and Conditions (https://onlinelibrary.wiley.com/terms-and-conditions) on Wiley Online Library for rules of use; OA articles are governed by the applicable Creative Commons License

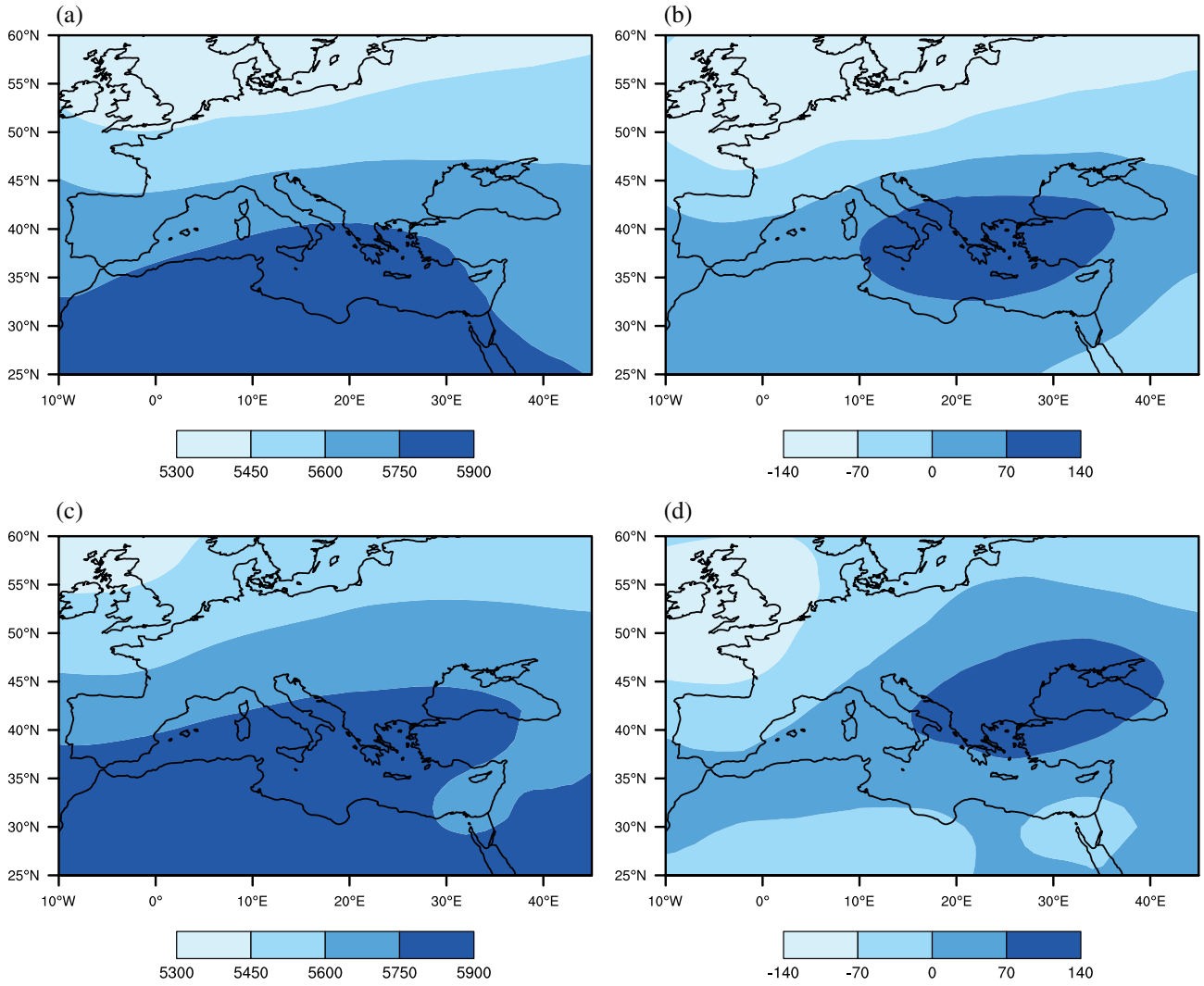

Figure 1. (a) Mean 500 hPa geopotential height (gpm) for 24–28 June 2007; (b) composite 500 hPa geopotential height anomaly for 24–28 June 2007; (c) as in (a), but for 20–27 July 2007; and (d) as in (b), but for 20–27 July 2007. [Colour figure can be viewed at wileyonlinelibrary.com].

temperature anomalies indicate that the largest anomalies are a departure of 5σ from the 1979–1999 climate mean.

3.2. Atmospheric-blocking analysis

Persistent blocking anticyclones greatly contribute to heat accumulation during hot summers. A blocking region hints at two important points: (1) hot-air temperatures are carried from the hot and dry North Africa; and (2) cooler circulation patterns are blocked on the northwest and not allowed to enter over the area where strong anticyclonic conditions maintain and sustain hot air temperatures.

The analysis of atmospheric blocking of the June 2007 period indicates that the blocking area extends from southeast of the Mediterranean to west of Turkey (Figures 3(a, b)). There is a major episode of atmospheric blocking in the eastern Mediterranean (Figure 3(a)). The total duration of the episode of atmospheric blocking (Figure 3(b)) reveals that anticyclonic conditions persisted over the area for about a week. There were also several instantaneous atmospheric-blocking events, which were around 16–18% over Turkey (not shown). They indicate the presence of atmospheric blocking throughout June 2007 and their impact on surface temperature can be inferred from Figures 2(a, b).

Studies of atmospheric blocking in the July 2007 period show much more pronounced atmospheric-blocking activity and the area being affected extends from the southwest Mediterranean to over northwest Turkey (Figures 3(c, d)). The area of the episode of atmospheric blocking extends from the southeastern Mediterranean to over the northwestern Black Sea and further north (Figure 3(c)). The analysis of duration of this episode of blocking indicated that the Balkans and northwest of Turkey were under persistent atmospheric-blocking conditions for 10–12 days. Over the same area, many instantaneous atmospheric-blocking events (38–40%) occurred. The effect of persistent blocking resulted in soaring temperatures over Turkey (Figures 2(c, d)).

3.3. Heat wave analysis

The HW detection technique outlined above in Section 2.1 was applied to the 2007 HW event. Initial analysis focuses on the total impact of the 2007 HW: (1) total number of HW days; (2) the number of HW occurrences; and (3) severity and (4) intensity of the HW event. This is followed by a detailed examination of

© 2018 Royal Meteorological Society

14698080, 2018, 3, Downloaded from https://rmets.onlinelibrary.wiley.com/doi/10.1002/met.1708 by NASA Shared Services Center (NSSC), Wiley Online Library on [26/05/2025]. See the Terms and Conditions (https://onlinelibrary.wiley.com/terms-and-conditions) on Wiley Online Library for rules of use; OA articles are governed by the applicable Creative Commons License

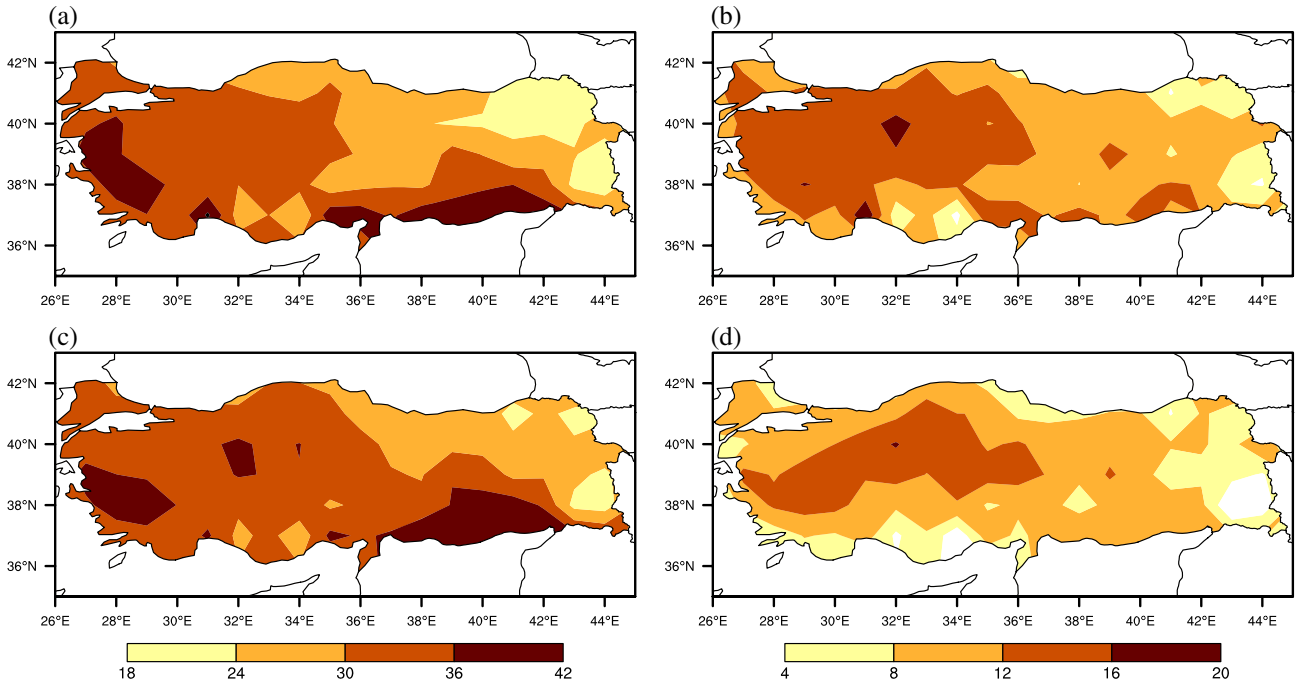

Figure 2. (a) Mean 2 m temperature (°C) for 24–28 June 2007; (b) 2 m temperature anomaly for 24–28 June 2007; (c) as in (a), but for 20–27 July 2007; and (d) as in (b), but for 20–27 July 2007. [Colour figure can be viewed at wileyonlinelibrary.com].

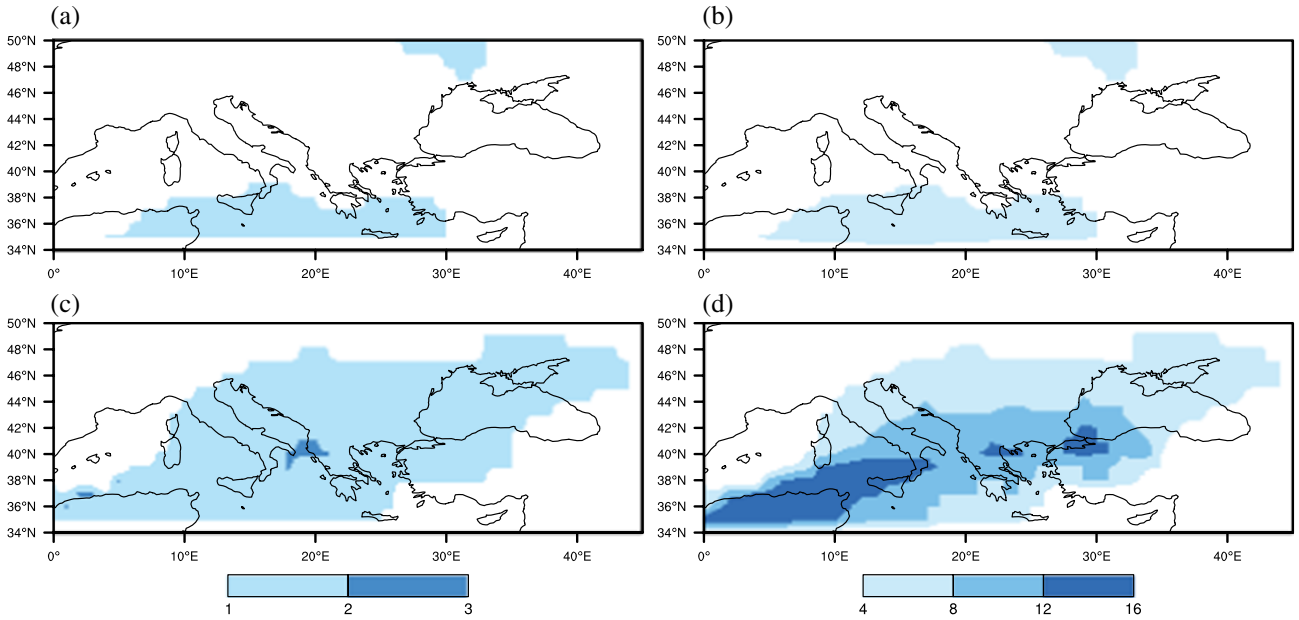

Figure 3. (a) Number of episode of atmospheric blocking for June 2007; (b) duration of the episode of blocking for June 2007; (c) as in (a), but for July 2007; and (d) as in (b), but for July 2007. [Colour figure can be viewed at wileyonlinelibrary.com].

each month to shed a light on the major characteristics of each HW episode.

The analysis of the June–July 2007 total number of HW days shows that the west of Turkey was under hot weather conditions for 20–36 days (Figure 4(a)). The region was hit by two to four HWs (Figure 4(b)). The HW severity analysis indicates that the west coast of Turkey was affected the most (Figure 4(c)). The intensity of HWs was determined by dividing severity over the number of HW days, and the results are presented in Figure 4(d). Intensity analysis reveals that it is over 1.5–3.5 °C in some places. Figure 4 as a whole highlights how the Aegean coastal side of Turkey has been affected by the 2007 HW, and how the other parts have not suffered as much. The 2000, 2010 and 2016 HWs affected Turkey extensively, but the 2007 HW differs from them in terms of its spatiotemporal extent (as shown in Figure S6 in the supplemental data online).

The year 2007 HW episodes were analysed individually to have more in-depth insight of each HW period. The analysis of the June 2007 period reveals that southwestern coastal locations had 8–20 HW days, and in some other places the duration of

© 2018 Royal Meteorological Society

14698080, 2018, 3, Downloaded from https://rmets.onlinelibrary.wiley.com/doi/10.1002/met.1708 by NASA Shared Services Center (NSSC), Wiley Online Library on [26/05/2025]. See the Terms and Conditions (https://onlinelibrary.wiley.com/terms-and-conditions) on Wiley Online Library for rules of use; OA articles are governed by the applicable Creative Commons License

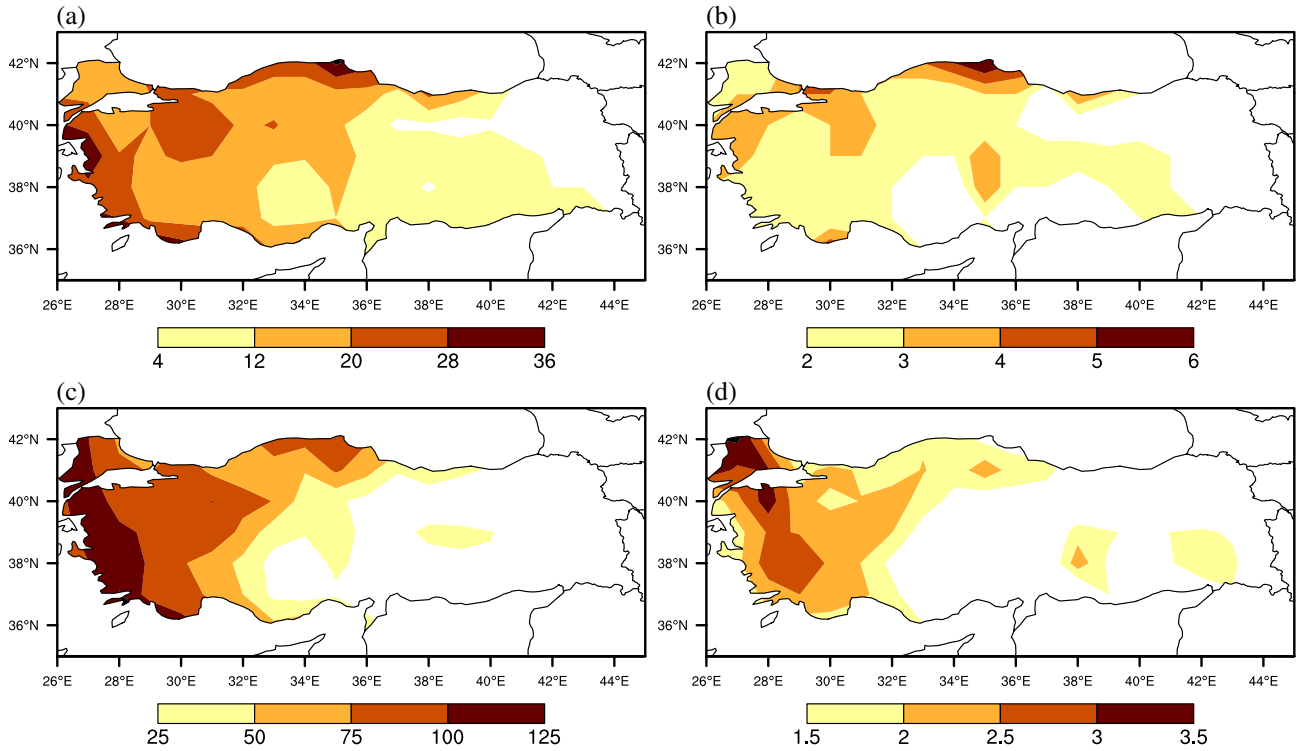

Figure 4. For the June–July 2007 period: (a) total number of heat wave (HW) days; (b) total number of HW; (c) HW severity (°C); and (d) HW intensity (°C). [Colour figure can be viewed at wileyonlinelibrary.com].

HWs was around 4–8 days (Figure 5(a)). In terms of the number of HW activities, one major HW event affected most parts of the country, but in a few places there were two HW events (Figure 5(b)). HW intensity is the highest on the northwest, which shows 3–5 °C (Figure 5(c)). The salient features of the June 2007 HW are in line with the position and magnitude of the 500 hPa geopotential anomalies (Figure 1(b)), the 850 hPa composite temperature anomalies (as shown in Figure S5 in the supplemental data online) and the June 2007 SST anomalies (as shown in Figure S4, also online). The June 2007 HW covered a smaller area and lasted for a shorter period; this may possibly be attributable to the position and duration of the June 2007 atmospheric-blocking episode (Figures 3(a, b)).

The analysis of the July 2007 HW period showed that longer HWs (8–16 days) cover a much larger area compared with the June 2007 HW period (Figure 5(d)). The total number of HW activities is similar to June 2007, but the affected area is larger (Figure 5(e)). The intensity of the July 2007 HW episode is not as large as that of the June 2007 HW episode over the same affected domain (Figure 5(f)). The July 2007 HW covered a larger area and lasted longer, which is in line with the position and duration of the July 2007 atmospheric-blocking episode (Figures 3(c, d)).

The decadal trend analyses of the total number and duration of HWs indicate an increase over the western and northwestern parts of Turkey, in particular for the 1998–2016 period, show the most increase (as shown in Figures S7 and S8 in the supplemental data online) and the 2007 HW is in line with this increased trend of this period. Previous HW studies of observed temperatures referred to western Turkey and the Turkish Black Sea coastline as hotspots of HW changes (Kuglitsch *et al.*, 2010). Studies focusing on Turkey highlight a rise in temperature (Erlat and Türkeş, 2013) and a rising trend in HW occurrences over the western part of Turkey (Unal *et al.*, 2013). Regional climate projection studies also identify the Mediterranean region as the most responsive hotspots for increasing heat stress (Giorgi, 2006; Diffenbaugh *et al.*, 2007).

4. Summary and conclusions

The present study investigated the connection between the high temperatures of June–July 2007 and atmospheric-blocking events by using an objective heat wave (HW) detection method and an atmospheric-blocking detection method. The HW detection method provided an objective analysis of the HW episodes of June–July 2007 throughout different regions of Turkey, which otherwise would have required the use of spatially varying temperature threshold due to the variation in topography and microclimatic features across the country. This detection method can be useful for investigating the salient features of HW: their spatial distribution, duration, total number of HWs, severity and intensity. The position of atmospheric blocking has an impact on the strength and duration of HWs. The objective blocking-detection method used in this study has emerged as a valuable tool for representing the phenomenon. This method can be useful for investigating the spatial coverage and time persistence of blocking events important for the occurrence of temperature extremes.

Concurrent large-scale atmospheric developments and associated flow anomalies provided the conditions that were conducive to the June–July 2007 hot weather conditions. In order to analyse the 2007 HW from a dynamic point of view, the mean and composite anomalies of 500 hPa geopotential height and temperature at 2 m height, i.e. 24–28 June and 20–27 July 2007, were also analysed. The atmospheric conditions of June–July 2007 are characterized by the presence of consecutive episodes of pronounced anticyclonic circulations, which lead to the advection of very hot air masses from North Africa to over the

© 2018 Royal Meteorological Society

14698080, 2018, 3, Downloaded from https://rmets.onlinelibrary.wiley.com/doi/10.1002/met.1708 by NASA Shared Services Center (NSSC), Wiley Online Library on [26/05/2025]. See the Terms and Conditions (https://onlinelibrary.wiley.com/terms-and-conditions) on Wiley Online Library for rules of use; OA articles are governed by the applicable Creative Commons License

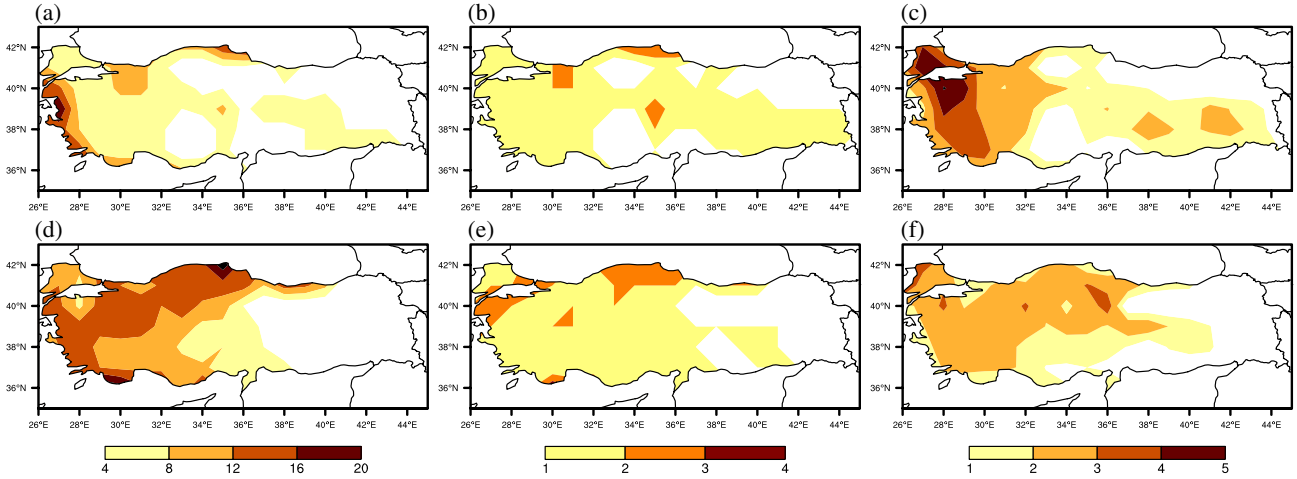

Figure 5. (a) Duration of heat waves (HWs) for June 2007; (b) number of HWs for June 2007; (c) HW intensity (°C) for June 2007; (d) as in (a), but for July 2007; (e) as in (b), but for July 2007; and (f) as in (c), but for July 2007. [Colour figure can be viewed at wileyonlinelibrary.com].

eastern Mediterranean and Turkey. The subsidence (which leads to intense adiabatic heating) and clear-sky conditions associated with a persistent high are the main cause of warm extremes, which resulted in temperatures having surpassed 40 °C in many places. Reduced soil moisture due to lack of precipitation could be another driving factor for the amplification of the 2007 HW. The analysis of June–July 2007 mean SST and composite anomalies highlighted higher-than-usual SSTs for each June HW episode, which might have positively contributed to the 2007 HW event.

Persistent atmospheric-blocking highs strongly influence surface temperature through circulation characteristics and associated radiative forcing. It was shown that atmospheric blocking occurred adjacent to the HW-affected region and played a key role in triggering and sustaining severe HW episodes. In June 2007, the blocking was located over the central Mediterranean and persisted for a week; in July 2007, it was southwest–northeast oriented and extended over the northwest of Turkey and lasted for 10–12 days.

HWs affected the Balkans and Turkey throughout June–July 2007. The analysis of the 2007 HW showed that the western coastal part of Turkey was affected the most. The total number of HW days ranged from 20 to 36 on the west coast, and three to four HWs hit this region. Other parts of the country were not affected as much. Individual analysis of the June and July 2007 HW episodes provided a detailed account of each episode. The June 2007 HW episode was shorter but the most intense, and confined to a smaller area on the west coast. The July 2007 HW episode covered a larger area and lasted longer, which coincided with the position and duration of the July 2007 atmospheric-blocking episode.

The link between the HIHWE and persistent atmospheric-blocking highs is important for both weather and the investigation of temperature extremes in the framework of climate variability. The occurrence of mega-HWs, for example the 2003 (Black *et al.*, 2004) and 2010 (Dole *et al.*, 2011; Matsueda, 2011) HWs, may increase in future. Climate-simulation studies project more intense, more frequent and longer-lasting HWs into the 21st Century (Meehl and Tebaldi, 2004). Society is faced not only with addressing current climate variability, but also with finding ways to adapt to future climate changes relating to the HIHWE. The present study does not address whether or not the summer of 2007 may resemble a summer in future decades over Turkey under climate-change scenarios, but this shall be investigated in a future study.

Acknowledgements

Meteorological data were obtained from the Turkish State Meteorological Service and the European Centre for Medium-Range Weather Forecasts. Plots were created using the National Center for Atmospheric Research (NCAR) Command Language (NCL, 2016). The author is very grateful to these organizations.

Supporting information

The following material is available as part of the online article:

Figure S1. Mean and anomaly of mean sea-level pressure.
Figure S2. Mean and anomaly of total precipitation.
Figure S3. Mean and anomaly of volumetric soil-water layer 1.
Figure S4. Mean and anomaly of sea-surface temperature.
Figure S5. Mean and anomaly of temperature at 850 hPa.
Figure S6. Duration of heat waves for the selected cases.
Figure S7. Trend of the duration of heat waves for selected periods.
Figure S8. Trends of the total number of heat waves for selected periods.

References

Barriopedro D, Fischer EM, Luterbacher J, Trigo RM, García-Herrera R. 2011. The hot summer of 2010: redrawing the temperature record map of Europe. *Science* **332**: 220–224.
Beniston M. 2004. The 2003 heat wave in Europe: a shape of things to come? An analysis based on Swiss climatological data and model simulations. *Geophys. Res. Lett.* **31**: L02202.
Black E, Blackburn M, Harrison G, Hoskins BJ, Methven J. 2004. Factors contributing to the summer 2003 European heatwave. *Weather* **59**: 217–223.
Cheval S, Dumitrescu A, Bell A. 2008. The urban heat island of Bucharest during the extreme high temperatures of July 2007. *Theor. Appl. Climatol.* **97**: 391–401.
Davini P, Cagnazzo C, Neale R, Tribbia J. 2012. Coupling between Greenland blocking and the North Atlantic Oscillation pattern. *Geophys. Res. Lett.* **39**: L14701.
Dee DP, Uppala SM, Simmons AJ, Berrisford P, Poli P, Kobayashi S, *et al.* 2011. The ERA-interim reanalysis: configuration and performance of the data assimilation system. *Q. J. Roy. Meteorol. Soc.* **137**: 553–597.

© 2018 Royal Meteorological Society

14698080, 2018, 3, Downloaded from https://rmets.onlinelibrary.wiley.com/doi/10.1002/met.1708 by NASA Shared Services Center (NSSC), Wiley Online Library on [26/05/2025]. See the Terms and Conditions (https://onlinelibrary.wiley.com/terms-and-conditions) on Wiley Online Library for rules of use; OA articles are governed by the applicable Creative Commons License

Demirtaş M. 2016. The October 2011 devastating flash flood event of Antalya: triggering mechanisms and quantitative precipitation forecasting. *Q. J. R. Meteorol. Soc.* **142**: 2336–2346.
Demirtaş M. 2017. The large scale environment of the European 2012 high-impact cold wave: prolonged upstream and downstream atmospheric blocking. *Weather* **72**: 297–301.
Diffenbaugh NS, Pal JS, Giorgi F, Xuejie G. 2007. Heat stress intensification in the Mediterranean climate change hotspots. *Geophys. Res. Lett.* **34**: L11706.
Dole R, Hoerling M, Perlwitz J, Eischeid J, Pegion P, Zhang T, *et al.* 2011. Was there a basis for anticipating the 2010 Russian heat wave? *Geophys. Res. Lett.* **38**: L06702.
Erlat E, Türkeş M. 2013. Observed changes and trends in numbers of summer and tropical days, and the 2010 hot summer in Turkey. *Int. J. Clim.* **33**(8): 1898–1908.
Feudale L, Shukla J. 2007. Role of Mediterranean SST in enhancing the European heat wave of summer 2003. *Geophys Res Lett.* **34**: L03811.
Feudale L, Shukla J. 2010. Influence of sea surface temperature on the European heat wave of 2003 summer, part II: a modelling study. *Climate Dynam.* **36**: 1705–1715.
Fischer EM, Seneviratne SI, Vidale PL, Lüthi D, Schär C. 2007. Soil moisture–atmosphere interactions during the 2003 European summer heat wave. *J. Clim* **20**: 5081–5099.
Founda D, Giannakopoulos C. 2009. The exceptionally hot summer of 2007 in Athens, Greece. *Global Planet. Change* **67**: 227–236.
Giorgi F. 2006. Climate change hot-spots. *Geophys. Res. Lett.* **33**: L08707. https://doi.org/10.1029/2006GL025734.
Kuglitsch FG, Toreti A, Xoplaki E, Della-Marta PM, Zerefos CS, Türkeş M, *et al.* 2010. Heat wave changes in the eastern Mediterranean since 1960. *Geophys. Res. Lett.* **37**: L04802.
Lorenz R, Jaeger EB, Seneviratne SI. 2010. Persistence of heat waves and its link to soil moisture memory. *Geophys. Res. Lett.* **37**: L09703.
Luterbacher J, Liniger MA, Menzel A, Estrella N, Della-Marta PM, Pfister C, *et al.* 2007. Exceptional European warmth of autumn 2006 and winter 2007: historical context, the underlying dynamics and its phonological impacts. *Geophys. Res. Lett.* **34**: L12704.
Marshall AG, Hudson D, Wheeler MC, Alves O, Hendon HH, Pook MJ, *et al.* 2014. Intra-seasonal drivers of extreme heat over Australia in observations and POAMA-2. *Climate Dynam.* **43**(7–8): 1915–1937.
Matsueda M. 2011. Predictability of Euro-Russian blocking in summer of 2010. *Geophys. Res. Lett.* **38**: L06801. https://doi.org/10.1029/2010GL046557.
Meehl GA, Tebaldi C. 2004. More intense, more frequent, and longer lasting heat waves in the 21st century. *Science* **305**: 994–997.
Miralles DG, Teuling AJ, van Heerwaarden CC, de Arellano VG. 2014. Mega-heatwave temperatures due to combined soil desiccation and atmospheric heat accumulation. *Nat. Geosci.* **7**: 345–349.
Perkins SE. 2015. A review on the scientific understanding of heatwaves–their measurement, driving mechanisms, and changes at the global scale. *Atmos. Res.* **164**: 242–267.
Pfahl S, Wernli H. 2012. Quantifying the relevance of atmospheric blocking for co-located temperature extremes in the northern hemisphere on (sub-)daily time scales. *Geophys. Res. Lett.* **39**: L12807.
Rebetez M, Dupont O, Giroud M. 2009. An analysis of the July 2006 heatwave extent in Europe compared to the record year of 2003. *Theor. Appl. Climatol.* **95**: 1–7.
Rex DF. 1950. Blocking action in the middle troposphere and its effect upon regional climate. I. An aerological study of blocking action. *Tellus* **2**: 196–211.
Robinson PJ. 2001. On the definition of a heat wave. *J. Appl. Meteorol.* **40**: 762–775.
Russo S, Dosio A, Graversen RG, Sillmann J, Carrao H, Dunbar MB, *et al.* 2014. Magnitude of extreme heat waves in present climate and their projection in a warming world. *J. Geophys. Res. Atmos.* **119**(12): 500–512.
Schär C, Vidale PL, Lüthi D, Frei C, Häberli C, Liniger MA, Appenzeller C. 2004. The role of increasing temperature variability for European summer heat waves. *Nature* **427**: 332–336. https://doi.org/10.1038/nature02300.
Scherrer S, Croci-Maspoli M, Schwierz C, Appenzeller C. 2006. Two-dimensional indices of atmospheric blocking and their statistical relationship with winter climate patterns in the Euro-Atlantic region. *Int. J. Climatol.* **26**: 233–249.
Scheuren JM, le Polain de Waroux O, Below R, Guha-Sapir D, Ponserre S. 2008. *Annual Disaster Statistical Review: The Numbers and Trends 2007*. CRED: Brussels.
Spinoni J, Lakatos M, Szentimrey T, Bihari Z, Szalai S, Vogta J, *et al.* 2015. Heat and cold waves trends in the Carpathian region from 1961 to 2010. *Int. J. Climatol.* **35**: 4197–4209.
Stefanon M, D'Andrea F, Drobinski P. 2012. Heatwave classification over Europe and the Mediterranean region. *Environ. Res. Lett.* **7**: 014023.
The NCAR Command Language (Version 6.3.0) (Software). 2016. Boulder, CO: UCAR/NCAR/CISL/TDD. https://doi.org/10.5065/D6WD3XH5.
Tibaldi T, Molteni F. 1990. On the operational predictability of blocking. *Tellus* **42A**: 34–365.
Unal YS, Tan E, Mentes SS. 2013. Summer heat waves over western Turkey between 1965 and 2006. *Theor. Appl. Climatol.* **112**: 339–350.
Vautard R, Yiou P, D'Andrea F, de Noblet N, Viovy N, Cassou C, *et al.* 2007. Summertime European heat and drought waves induced by wintertime Mediterranean rainfall deficit. *Geophys. Res. Lett.* **34**: L07711.
WMO – World Meteorological Organization. 2007. eStatement on the Status of the Global Climate in 2007. WMO-No. 1031, 16pp.

© 2018 Royal Meteorological Society

14698080, 2018, 3, Downloaded from https://rmets.onlinelibrary.wiley.com/doi/10.1002/met.1708 by NASA Shared Services Center (NSSC), Wiley Online Library on [26/05/2025]. See the Terms and Conditions (https://onlinelibrary.wiley.com/terms-and-conditions) on Wiley Online Library for rules of use; OA articles are governed by the applicable Creative Commons License